doi.org/10.36721/PJPS.2021.34.4.REG.1449-1458.1

Atractylenolide II induces cell cycle arrest and apoptosis in breast cancer cells through ER pathway

Shaohua Dou[1#], Chao Yang[1#], Danfeng Zou[3#], Wa Da[2], Muqaddas Masood[1], Salah Adlat[1], Yang-Jin Baima[2], MI Nasser[1]*, Bin Li[2]* and Nan Jiang[1,2]*

[1]Colleges of Life Science and Technology, Dalian University, Dalian Economic-Technological Development Zone, Liaoning, China
[2]Institute of Animal Husbandry and Veterinary, Tibet Autonomous Regional Academy of Agricultural Sciences, Lhasa, Tibet, China
[3]Huiqiao Medical Center, Nanfang Hospital, Southern Medical University, Guangzhou, China

Abstract: In this research, atractylenolide II (ATR II) on apoptosis, cell cycle cells via ER pathway in breast cancer (MDA-MB-231 and MCF-7) cells are assessed. The effect of ATR II on cell proliferation was detected by MTT assay. Additional flow cytometry, luciferase, the western blot were performed to detect the signaling pathway cytotoxicity of ATR II. We have also carried out autodock measurements to validate our results. Our findings showed ATR II could inhibit breast cancer cell growth by apoptosis mainly through G2/M-phase cell cycle arrest. Besides, the cytotoxicity of ATTR II on breast cancer was also correlated by the regulation of endrogen receptors and promising an anti-inflammatory activity via inhibiting NF-KB signaling pathways. Taking together, ATR II could be a potential anti-cancer drug for breast cancer.

Keywords: ATR II, apoptosis, ER/NF-KB, G2/M, autodock.

INTRODUCTION

Breast cancer is one of the most severe heterogeneous diseases leading to millions of deaths every year (Bray *et al*. 2018). Different efforts have been devoted to overcoming this critical issue by paying particular attention to its prevention, diagnosis, and treatment. Breast cancer can be treated through surgery, chemotherapy, or radiotherapy methods, which differ in their actions (Currey *et al*. 2018; Ponde *et al*. 2018). Nevertheless, these approaches are practical only at the earlier stage of tumor activity. Furthermore, these strategies present little and short-term effectiveness because of their high toxicity, off-targeting effects, and inefficiencies for long-term use (Quintela-Fandino *et al*. 2017).

Previous studies have reported that more than 80% of breast cancers express estrogen receptors (ER). ER is further divided into ER-alpha (ERα) and ER-beta (ERβ) as a steroid hormone receptor. Szmyd *et al.* reported that ERα-positive cells had a higher number of normal breast cancer genes than ERα-negative cell lines in an estrogen-dependent manner (Szmyd *et al*. 2018). Studies also showed that overexpression of ER-β and inhibition of ERα could be an effective anti-tumor strategy against breast cancer (De Luca *et al*. 2015; Park and Lee 2014; Qi *et al*. 2005). In addition, the level of nuclear factor kappa-B (NF-κB) is elevated in ER-human breast cancers compared with ER^+ cells. Moreover, several studies have reported a high ratio of the nuclear factor kappa-B (NF-κB) in ER^-human breast cancers compared with ER^+ cells. The transcription factor NF-κB is a crucial factor in regulating immune system responses associated with cancer. In its inactive form, NF-κB remains in the cytoplasm with its protein inhibitors (IκBs). External stimuli such as tumor necrosis factor might drive the phosphorylation of IκBα at its serine 32 or 36 part through IκB kinase that consequently translocates NF-κB from the cytoplasm to the nucleus. Furthermore, previous studies reported that in prostate cancer, cell line inhibition of ER-β induces suppression of inflammatory activity as well as NF-κB (Ashour *et al*. 2018; Dondelinger *et al*. 2015; Xiao *et al*. 2019). inflammatory and antioxidant activities because of their ability to regulate the activity of molecular targets as well as their signaling pathways, which are related to cell differentiation (Losada-Echeberria *et al*. 2017). Among them, sesquiterpene lactones have gained more attention due to fewer side effects (Samin *et al*. 2018). Atractylenolide II (ATR II) is a sesquiterpene derivative of the *Atractylodes chinensis* plant. ATR II was reported to have promising anti-tumor activity, notably in gastric cancer, colorectal cancer, and melanoma cell lines, through several signaling pathways (Ho Lin *et al*. 2016; Tian and Yu 2017; Ye *et al*. 2011). Furthermore, the biological efficiency of ATR II was reported by scientist; Indeed ATR has been shown to possess antioxidant, anti-inflammatory, Neuroprotective among other (Hossen *et al*. 2019; Yim *et al*. 2018).

Despite its biological effectiveness against different cancer cells, the molecular mechanism by which ATR II affects benign and malignant breast cancer cells has not been studied. Therefore, this study aimed to utilize ATR II

**Corresponding author:* e-mail: jiangnan678@sohu.com

[#]These authors contributed equally to this work.

as an anti-cancer agent to cure breast cancer malignant and benign by determining the functional mechanism of ATR II against breast cancer. Therefore, we hypothesized that ATR II could induce apoptosis in MCF-7 and MDA-MB 231 by regulating ER expression after stimulation of the androgen receptor through regulating the NF- signalling pathway.

MATERIALS AND METHODS

Cell Culture

Human Breast cancer cells MCF-7 and MDA-MB 231 and human mammary epithelial MCF 10A cultured and maintained in a DMEM medium containing 10% fetal bovine serum (Gibco, P.R. China). MCF-10A cells were cultured in DMEM/F12 (1:1) media supplemented with 5% horse serum, 1% PS, 0.05% hydrocortisone, 0.1% human insulin, 0.02% epidermal growth factor, and 0.01% cholera toxin. Cells were culture then; the cells were incubated at 37℃ in a humidified atmosphere of 5% CO2 and allowed for the growth of 70-80% of their confluent (Balhouse *et al*. 2017).

Cell proliferation assay

The cells were seeded on 96-well plates at a density of $3\times104ml^{-1}$, with 100 L per well. After the cells adhered to the wall, the medium was absorbed, and a drug-containing medium with different concentrations (0, 6, 12.5, 25, 50, 100, and 200μM) of ATR II was added, respectively. After 72h of culture, 25L of MTT solution of $5mg/ml^{-1}$ was added to each well and incubated for 4h. Then, the supernatant was discarded, and 200L of DMSO was added, determined at the wavelength of 490nm with an enzyme marker absorbance value. The proliferation inhibition rate was calculated according to formula (1).

I % = A570 (control) - A570 (treated)] / A570 (control) x 100.

Where I is the inhibition rate, and A is the absorbance at 570nm

Annexin V/PI assays for apoptosis

The apoptotic cells were investigated by annexin V/PI followed by flow cytometric regarding the manufacture protocol. MCF-7 and MDA-MB 231 cells (5×10^3 cells/well) were cultured in 6 wells plates and treated with different concentrations (0, 35, and 70) μM of ATR II 48h. After, cells were washed twice with PBS and stained with 5μL of Annexin V-FITC (Beyotime Institute of Biotechnology, China, #Cat. No.: C1062L) and 10μL of PI in 500μL binding buffer for 15min at room temperature in the dark. Finally, the apoptotic cells were determined by flow cytometry (Cytomics FC 500; Beckman Coulter Inc., Miami, FL)(Nasser *et al*. 2017).

Determination of MCF-7 and MDA-MB 213 cells cycle distribution

Cells were seeded in a 6-well plate with 2×10^5 mL^{-1} cells. After the cells adhered to the wall, different concentrations (0, 35 and 70μM) of ATR II were added to the plate for 48h. Further, the cell was collecting centrifugal gently with PBS suspension then fixed with 70% ethanol. After war cells, adjust cell concentration of 1 x, 10^6 mL, 1, with PBS wash liquid before dyeing, with 10μl RNase, 37℃ water bath for 30 min, then add 25 μl staining and mixed 4℃ avoid light than indicated at RT for 30 min. Flow cytometry instrument observation determined the cell cycle distribution (Nasser *et al*. 2017; Wang *et al*. 2018).

Determination of ROS expression in MCF-7 and MDA-MB 231 cells

To determine the generation of ROS production, cells were seed in 6 wells plate, then treated with or without 5mM N-acetylcysteine (NAC) and natural inhibitor of ROS. Afterward, cells were treated with different concentrations of ATR II for 48h. Finally, cells were harvested, washed, and resuspended in PBS containing 10μM of DCFH-DA for 15 minutes. The result was carried by flow cytometry analysis (Fengjiao *et al*. 2019).

Determination of Mitochondrial Membrane expression (MMP)

Cells with final concentrations of (0, 35 and 70) μM for 48 h were collected after 48 h treatment, then resuspended in 5001 diluted Rho 123 staining solution, centrifuged at 2000 r/min for 5min, washed twice with PBS, and resuspended again in PBS for flow cytometry detection (Wang *et al*. 2018).

Western-blot analysis

The MDA-MB-231 cells were inoculated into a 6-well plate at a density of 1×10^4 mL^{-1} cells per well, and the cells were treated with (0, 35, and 70) μM of ATR II for 48 h. The total protein was extracted with a total protein extraction kit and quantified with a BCA protein concentration determination kit. Then, the western-blot analysis was carried out by referring to the method of (Nasser *et al*. 2018) with a small modification. Chemi-doc MP was used to visualize the immune complex by chemiluminescence detection. Proteins were quantified using bio-RAD image analysis software, with -actin as sample control.

Real-time qPCR analysis

After 48 h, the cells were collected, and total RNA was extracted using the Eastep Super total RNA extraction kit. After the RNA was prepared, the No Script Reverse Transcription Mix kit and random primers were used (see table 1) for reverse transcription. PCR reaction conditions refer to qPCR Master Mix. ERβ, ERα, gene expressions were determined by ABI7500 rapid real-time PCR system, and β-actin was used as the control. The results of this experiment are expressed as "RQ" The results of this experiment are expressed as "RQ."

Gene	Forward (5'-3')	Reverse(5'-3')
ERβ	AATTCAGATAATCGACGCCAG	GTGTTTCAACATTCTCCCTCCTC
ERα	TAGTGGTCCATCGCCAGTTAT	GGGAGCCAACACTTCACCAT
β-actin	CACGATGGAGGGGCCGGACTCATC	TAAAGACCTCTATGCCAACACAGT

Transient Transfection and Luciferase Report

Cells were cultured in 48 well plates for 16 h, then transfected with NF-κB reporter (SA Biosciences) 100 ng in the presence of *Renilla* Luciferase control pREP7 vector 25 ng. Afterward, cells were treated with different concentrations of ATR II and incubated for 24 h.

Docking system test

3D structures of ATR II were obtained from NCBI PubChem. The crystal structure of DR4 (PDB code：1D5M) caspase-3 (PDB code: 1CP3) caspase 8 (PDB code : 1F9E), p53 (PDB code: 1A1U) ER-β (PDB code：1l2j), ER-α (PDB code：1A52), TNF-α (PDB code: 1A8M), Bax (PDB code : 1F16), and Bcl-2 (PDB code: 1G5J) were obtained from the Protein Data Bank. The ligands within the crystal structure complex were extracted by PyMOL software (San Carlos, CA, USA). AutoDock 4.2 version was used for the docking system test. AutoDock Tools initialized the ligands via adding gasteiger charges, merging non-polar hydrogen's, and setting rotatable bonds. The ligands were rewritten into PDBQT format, which can be read by Autodock software. AutoDock Tools were used to add polar hydrogen to the whole receptor. The grid box was set to contain the whole receptor region. The receptor output was also saved in PDBQT format. AutoDock Vina was set with the macromolecule held fixed and the ligands flexible. Affinity maps for all the atom types present and an electrostatic map and an electrostatic map were computed, with a grid spacing of 0.375Å. The structural models were collected from the lowest-energy docking solution of each cluster of AutoDock. Lower-binding energy indicates a stronger binding ability (binding energy between -5 to -10 are considered to have better binding affinity). (Nasser *et al*. 2020)

STATISTICAL ANALYSIS

Data were analyzed by the Statistical Pack-ages for Social Sciences (SPSS) software version 20.0 (IBM Inc., New York, USA). Results were expressed as mean ± standard deviation (SD). Significant differences between groups were evaluated using Student's *t* test. P-values were two-sided and P-values < 0.05 were considered statistically significant.

RESULTS

Cytotoxicity of ATR II

To underline the cytotoxicity of ATR II on the breast, we first compare its cytotoxicity with one breast normal and the cancer cell through the MTT assay. The cells were treated with 0, 6, 12.5, 25, 50, 100, and 200 µM concentrations of ATR II. As shown in fig. 1, ATR II was able to inhibit the proliferation of MCF-7 considerably, MDA-MB 231, cells, with consequently their half minimum concentration IC_{50} of, 70 and 68 µM.

ATR II induces apoptosis in MCF-7 and MDA-MB 231 cells

To verify whether the cytotoxicity induction by ATR II was associated with apoptosis, we performed a flow cytometric of annexin V-FITC and PI double-staining to quantitatively assess the early apoptosis (B4), late apoptosis (B2), and necrosis (B1). As shown in fig. 2A, the (B4) values increased with the rise of the ATR II concentration, respectively, in MCF-7 and MDA-MB 231 cells. Furthermore, a western blot was conducted to evaluate the caspase's activity. As illustrated in fig. 2B, ATR II can stimulate the activation of caspase-8, which would lead to activate caspase-3 consequently.

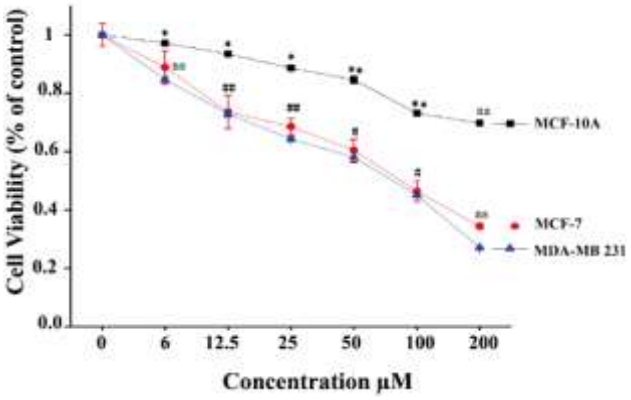

Fig. 1: Cytotoxicity of ATR II breast normal and cancer cells line: Cells line was treated with 0, 6, 12.5, 25, 50, 100, and 200µM of ATR II; Proliferation was assessed after 72h, as described in materials and methods. Each bar represents the mean ± standard deviation of three experiments*p<0.05 and **p<0.01 compared with the control.

To further comprehend the extrinsic-apoptosis mediate by ATR II in MCF-7 and MDA-MB 231 cells, we simulated the molecular binding of ATR II to death receptors or DR4, caspase-8, and caspase-3 by AUTO-DOCK calculations. The result warranted that ATR II was able to dock to all DR4 and caspase-8/3. As shown in fig. 2C, ATR II was surrounded by amino acids of DR4 with the lowest binding energy of -7.99Kcal/mol gained (LYS207, PHE208, ASP209, LYS212 and TYR213,). While ATRII was surrounded by six amino acid of caspase-3 with the lowest binding energy of -7.145Kcal/mol gained (THR77, ASN80, LEU81, ALA227, LYS224, and LEU233); finally,

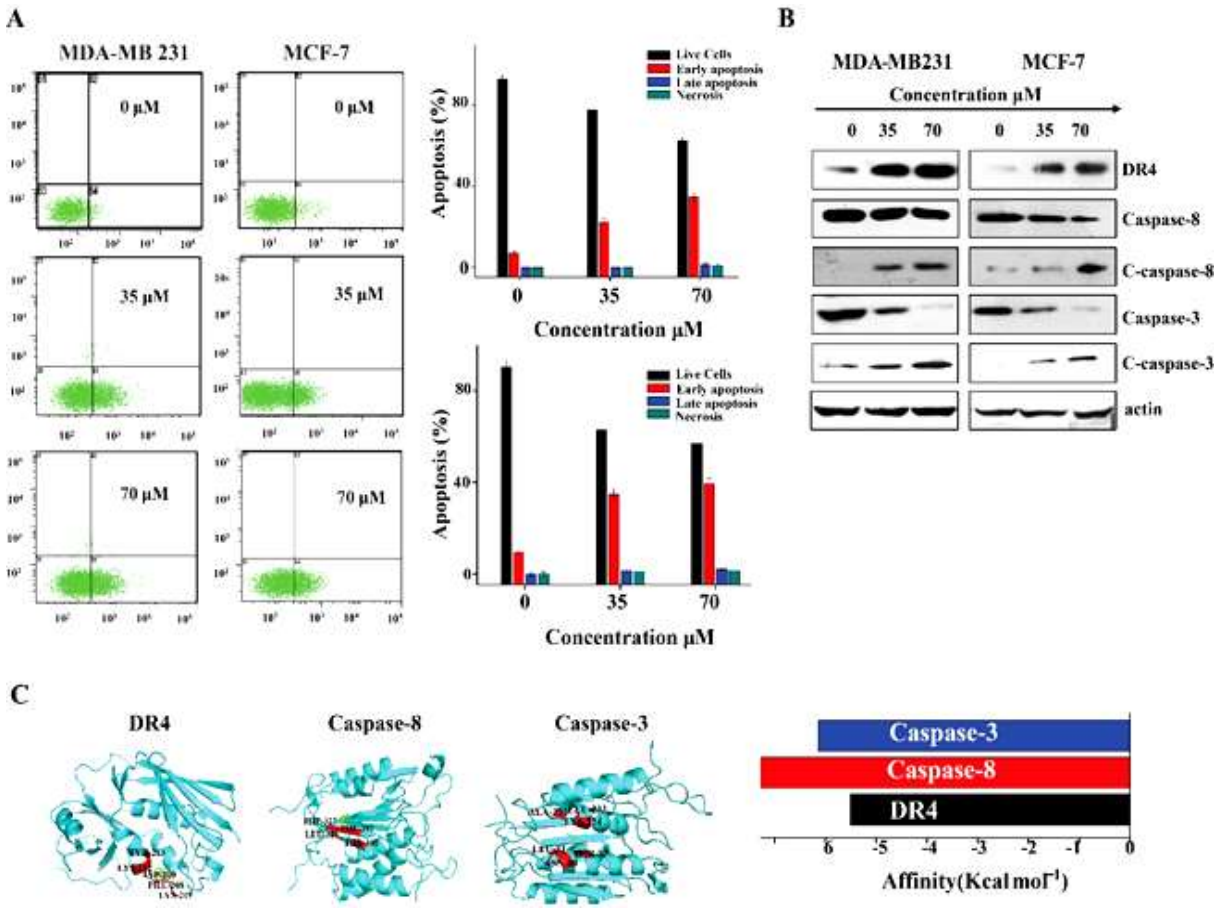

Fig. 2: Mechanism of induction of apoptosis by ATR II on MCF-7 and MDA-MB 231 cells. (A) MCF-7 and MDA-MB 231cells were subject to ATR II (0, 35 and 70µM) then, stained with annexin V /PI apoptosis assays through flow cytometry; the ratios of apoptotic cells to all cells were quantified based on three independent experiments compared with the control). (B)The cellular proteins were extracted to detect the levels of DR4, Caspase-8 and Caspase-3, as well as beta-actin (control) by Western blotting. (C) DR4, caspase3 and caspase-8 binding sites, as well as binding energy, were evaluated through AUTO-DOCK calculations.

we found that ATR II was also able to dock caspase-8 protein with the lowest binding energy of -7.28 gained, and ATR II was surrounded by six amino acid of caspase-8 (PHE327, LEU328, THR393, THR390, LEU329, and PHE392). These findings verify our hypothesis that ATR II presents the potential to induce apoptosis through extrinsic mitochondrial pathways.

ATR II promotes MCF-7 and MDA-MB 231 cells apoptosis through ROS induction and the collapse of mitochondrial membrane potential

In cancer cell lines, reactive oxygen species play a dual role (Shrivastava *et al*. 2014). In non-cancerous cells, ROS production rate remains low compared to the cancer cells in which stimuli such as inflammation lead to an overexpression of ROS in cells that conduct cell death by apoptosis autophagy (Kalyanaraman *et al*. 2018). A previous study reported that ATR II owned anti-inflammatory and anti-oxidative responses (Wang et al. 2017); therefore, we hypothesize whether it might act as a ROS inhibitor. Herein to underline whether the apoptosis induced by ATR II was associated with ROS induction in MCF-7 and MDA-MB 231 cells. Cells were treated with 0, 35 and 70µM of ATR II for 48h followed by the treatment with the fluorescent probes DCF-DA to detect and assess H_2O_2 by flow cytometry in the presence and absence of N-acetyl-cysteine (NAC). The outcomes showed that the generation of intracellular H_2O_2 improved considerably with ATR II treatment (0, 35, and 70) µM. In the meantime, NAC treatment resulted in regulating the induction of ROS expression due to treatment with different concentrations of ATR II (35 and 70 µM) correspondingly, which therefore depicted the role of ATR II in the generation of H_2O_2 as illustrated in fig. 3A.

A loss in the mitochondrial transmembrane potential ($\Delta\psi m$) has been observed due to the disruption of these counterbalances (Sun *et al*. 2016). To validate whether the apoptosis induced by ATR II was associated with mitochondrial depolarization, the investigation was conducted on MCF-7 and MDA-MB 231 cells through the employment of Rhodamine 123 staining flow cytometry.

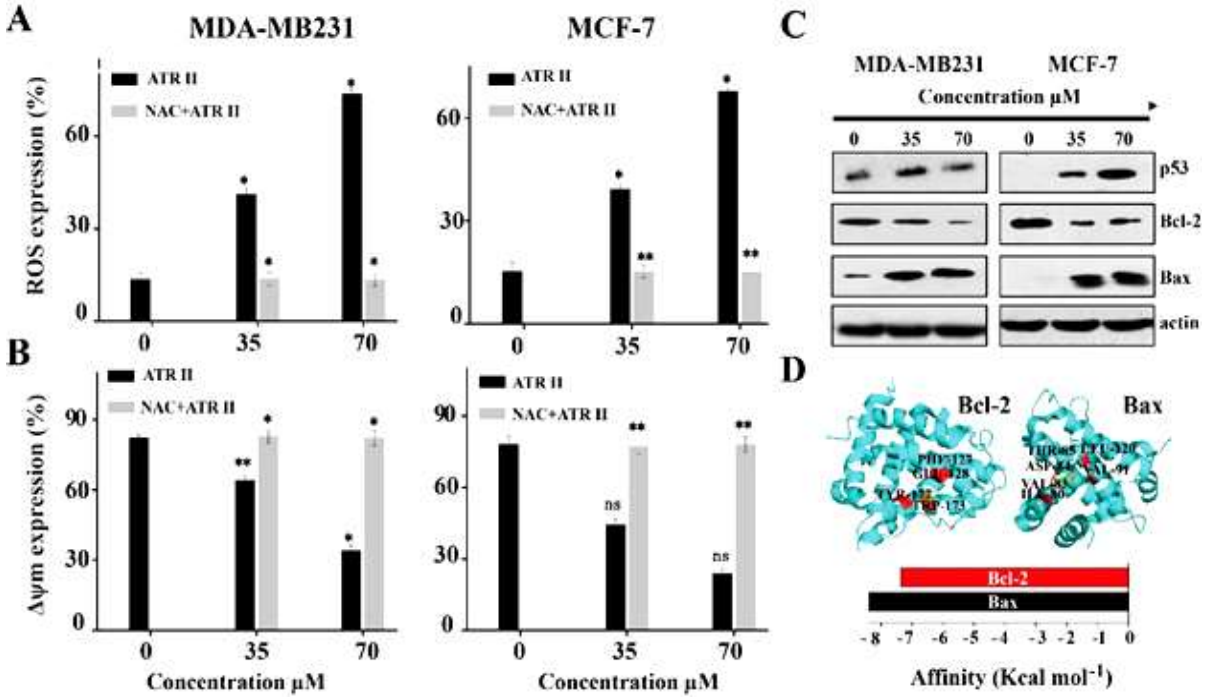

Fig. 3: ATR II induces apoptosis in MCF-7 and MDA-MB231 through overexpress oxidative stress (ROS), while collapsing Mitochondrial Membrane Potential, (A) Relative ROS generation in cells determined by DCFH-DA incubation and assessed via a fluorescence microplate reader. Data points represent the means ± SD, n = 3*p<0.05, and **p<0.01 versus control cells. (B) Relative Δψm generation in cells determined by Rhodamine 123 incubation and assessed via a fluorescence microplate reader. Data points represent the means ± SD, n = 3*p<0.05, and **p<0.01 versus control cells. (C) Relative protein expression controlling the mitochondrial membrane potential assess through western blot compare with control beta-actin. (D)Bcl-2 and Bax binding site, as well as binding energy, was evaluated through AUTO-DOCK calculations.

ATR II showed to induce mitochondrial membrane potential collapse in dose depend-manner. However, the pre-treatment of MCF-7 and MDA-MB 231 cells with NAC completely reverse the action of ATR II (fig. 3B).

As shown in fig.3C, treatment of MCF-7 and MDA-MB 231 cells by ATR II would induce mitochondrial membrane potential loss. This fall of mitochondrial membrane potential was mainly caused by the capability of ATR II to activate tumor suppressor p53; proteins were shown in fig. 3B. To further make sense of the previous result, we simulated the molecular binding of ATR II Bax and Bcl-2 by AUTO-DOCK calculations. As shown in fig. 3D, ATR II was able to dock to both Bcl-2 and Bax protein structures. Indeed, ATR II was surrounded with eight amino acids of Bax, and the lowest binding energy of -7.36Kcal/mol was gained (ILE80, VAL83, ASP84, THR85, PRO88, VAL91, PHE116, and LEU120). Likewise, four amino acids of Bcl-2 and the lowest binding energy of -8.4Kcal/mol were gained (PHE127, GLU128, TRP173, and TYR177) the docking structure.

ATR II induces apoptosis through phosphorylation of NF-κB signaling pathways

The transcription factor, NF-κB, is a regulator of cell proliferation as well as cell death. Once it is activated, it will be translocated into the nucleus to induce activation of IκB and inhibition of IκB (House *et al*. 2018). Here, we assessed NF-κB signaling pathways through the use of ATR II treatment ultimately, whereas TNF-α receptors would target the phosphorylation of IκB and expression of NF-κB. Results showed a reduction in expression of IKK-α, COX-2, NF-κB, and TNF-α as illustrated in fig. 4A, these findings show that ATR II acts as an anti-inflammatory agent and an inducer of apoptosis in MCF-7 and MDA-MB 231 cells by inhibiting inflammatory factors.

To provide further evidence of ATR II role in NF-κB regulation, we conduct transient Transfection and Luciferase tests in MCF-7 and MDA-MB 231 cells. We found that ATR II significantly inhibits NF-κB expression in MCF-7 and MDA-MB 231 cells (fig. 4B). Furthermore, the role of ATR II in the phosphorylation of inflammatory factors was examined through the molecular binding simulations of ATR II by NF-κB and TNF-α by AUTO-DOCK calculation. Results warranted that ATR II was able to dock on both NF-κB and TNF-α protein structures. ATR II was surrounded with four amino acids of TNF-α, with the lowest binding energy of -8,76Kcal/mol was gained (LEU26, TRP28, ASN46, and ALA134). While ATR II was surrounded by four amino

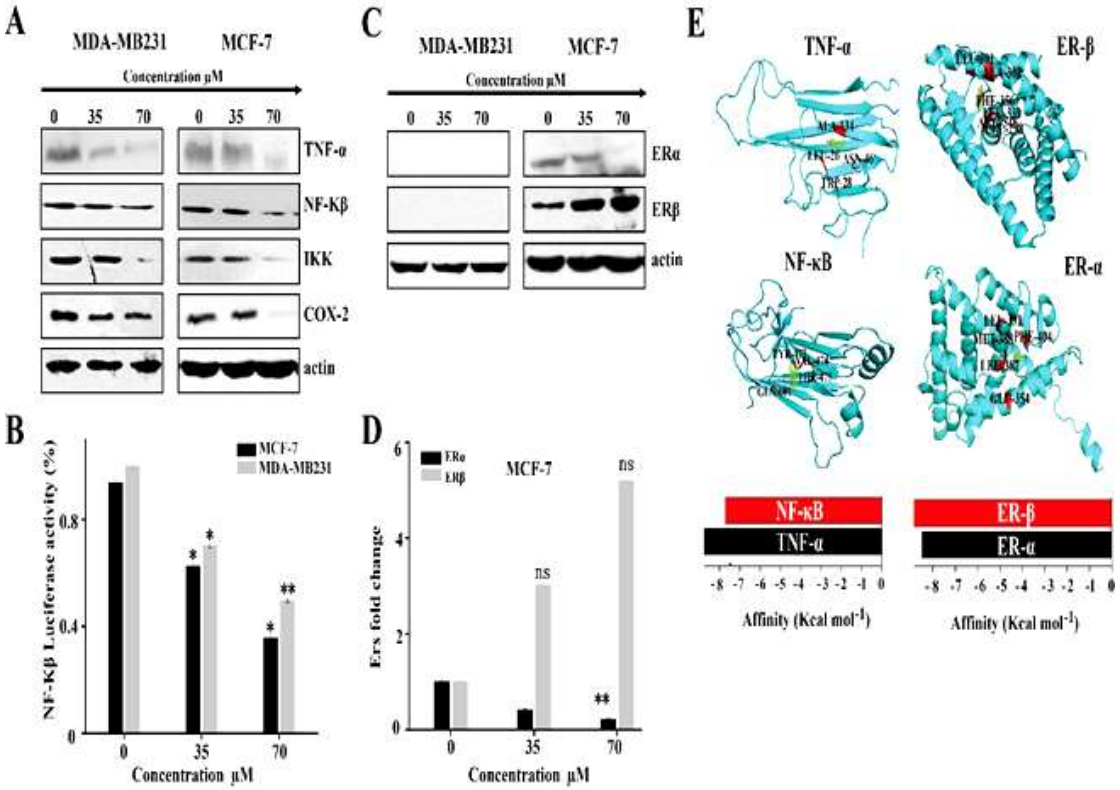

Fig. 4: ATR II induces MCF-7 and MDA-MB 231 cells apoptosis through the regulation of NF-κB/ER pathways. (A) Cells were treated with or without ATR II (0, 35, and 70 μM) for 48 h. The cellular proteins were extracted to detect the levels of NF-κB, IKK-α, COX-2, and beta-actin (control) by Western blotting. (B) MCF-7 and MDA-MB 231 cells were transiently transfected NF-κB luciferase reporter plasmid. Cells were treated with ATR II (0, 35, and 70 μM) for 24h and then harvested for luciferase assays. (C) MCF-7cells were treated with or without ATR II (0, 35, and 70 μM) for 48h. The cellular proteins were extracted to detect the levels of ERα and ERβ as well as beta-actin (control) by Western blotting. (D) Real-time RT-PCR was used to quantify the ERα and ERβ mRNA levels in MCF-7 cells following 48 h treatment of ATR II (0, 35 and 70 μM). A fold decrease of gene expression was calculated by dividing the normalized gene expression activity by untreated control. The data shown are representative of three independent experiments with the similar results. *p<0.05; and **p<0.01 compared with the control. (E and F)TNF-α, NF-KB, ER-α and ER-β binding sites and binding energy, were evaluated through AUTO-DOCK calculations.

acids of NF-κB protein, the lowest binding energy of -7.72Kcal/mol was gained (TYR473, VAL474, THR475, and GLN601) in the docking structure (fig. 4E).

ATR II induce ER-β Up-regulation and ERα Down-regulation in MCF-7 cells line

Different from ERα, ER-β is somewhat uncertain in the resistance of breast cancer. In consideration of the discrepancy, this study was planned to analyze the expression and function of ERα and ER-β on MCF-7 (ER-positive) and MDA-MB231 (ER-negative) via western blot. As shown in fig. 4C, ER-β expression was significantly up-regulated, whereas ERα is shown to be down-regulated in a dose-dependent manner in MCF-cells. In contrast, there was no ER expression in MDA-231 cells (fig. 4C). RT-PCR further testified the findings mentioned above (fig. 4D).

To further understand the effects of ATR II-mediated breast cancer cell death on ER, we simulated the molecular binding of ATR II by ERα and ER-β through AUTO-DOCK calculations. As shown in fig. 4F, ATR II was able to dock on both ERα and ER-β protein structures. ATR II was surrounded by six amino acids of ERα with the lowest binding energy of -8.48Kcal/mol gained (GLU354, LEU387, ARG394, MET388, LEU391, and PHE404). While ATR II was surrounded by eight amino acids of ER-β protein with the lowest binding energy of -8.84Kcal/mol was gained (LEU301, ALA302, LEU298, ARG346, LEU339, MET340, LEU343, and PHE356), in docking structure (fig. 4F).

ATR II induces G2/M phase cell cycle arrest in MCF-7 and MDA-MB 231 cells

Similar to apoptosis, cell death might occur by cell cycle arrest. To test whether the cytotoxicity of ATR II can influence cell cycle arrest, flow cytometry was conducted to evaluate particular disruptions induced by ATR II in the distribution of cell cycle of MCF-7 and MDA-MB 231 (fig. 5A). The G2/M phases increased in MCF-7 and

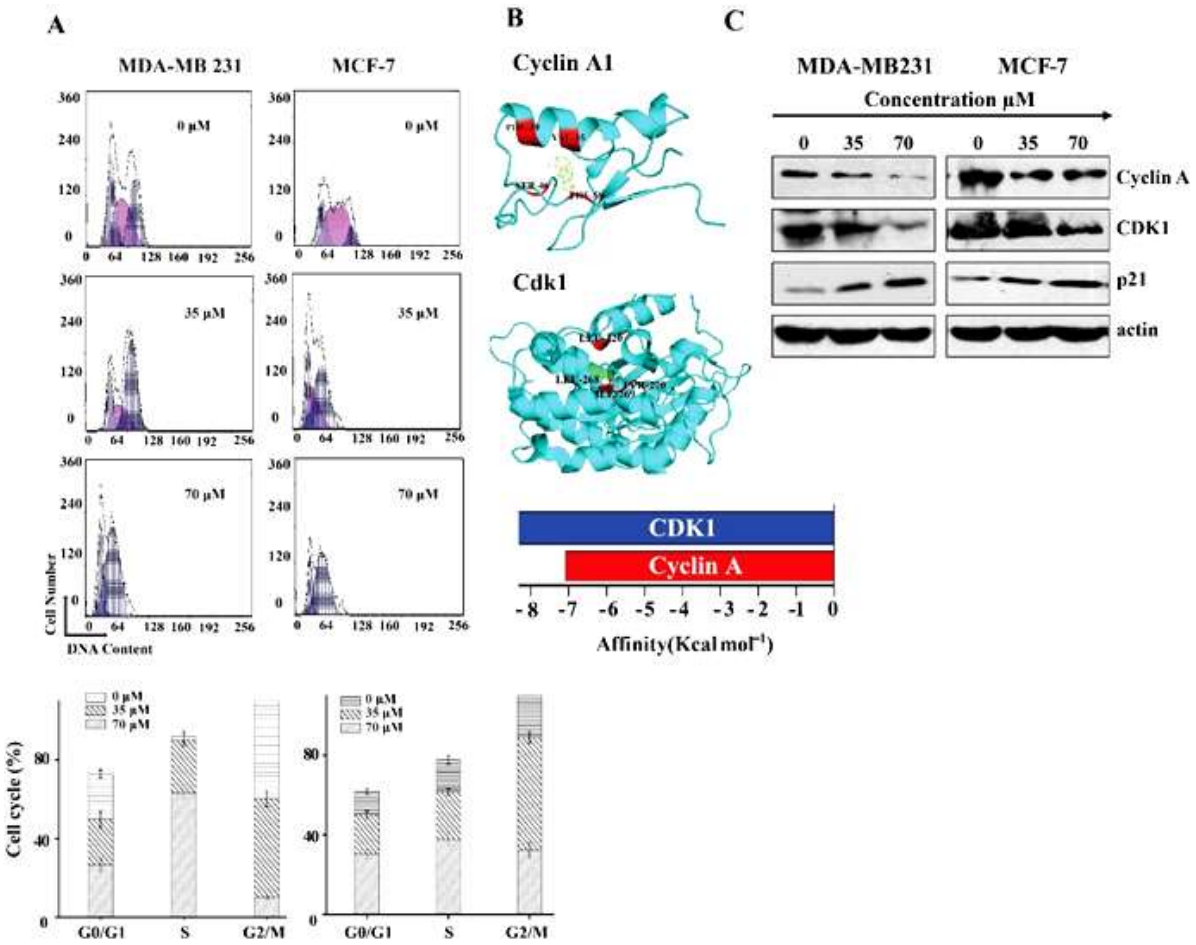

Fig. 5: ATR II induces MCF-7 and MDA-MB 231 cells cycle arrest at G2/M phase arrest) MCF-7 and MDA-MB 231cells were subject to ATR II (0,35 and 70μM) then, stained with annexin PI cell cycle assays trough flow cytometry, The ratios of a different phase of the cycle were quantified based on three independent experiments (*p<0.05; and **p<0.01 compared with the control). (B) MCF-7 and MDA-MB 231 Cells were treated with ATR II (0, 35, and 70 μM) for 48h. The cellular proteins were extracted to detect the levels of p21, Cyclin A, CDK1, as well as beta-actin (control) by Western blotting. (C) Cyclin and CDK1 binding site, as well as binding energy, was evaluated through AUTO-DOCK calculations.

MDA-MB 231 cells and decreased G0/G1 and S phases. Such results suggested that both MCF-7 and MDA-MB-231 cells cause cell cycle arrest in G2/M phases. A recent study [31] had reported that cell cycle arrest in MCF-7 and MBA-MD 231 cells occurs in the G2/M process; this arrest was regulated by the CDK1/Cyclin A complex and its downstream objective p21. Therefore, western blot tests were performed on the levels of p53, p21, Cyclin A, and Cdk1 protein expressions. Cyclin A and CDK1 were down-regulated by ATR II, and p21 and p53 expressions were up-regulated accordingly (fig. 5B). To verify that ATR II triggered G2/M arrest through inhibition of the CyclinA / Cdk1 complex, we simulated the molecular binding of ATR II, by CyclinA1 and Cdk1 by AUTO-DOCK calculations. ATR II was able to bind to both CyclinA1 and Cdk1 protein structures. ATR II was surrounded by four Cdk1 amino acids, which received the lowest binding power of -8,32Kcal/mol (LEU220, LEU268, IE268, and TYR270).

Likewise, four amino acids of CyclinA1 (PHE58, SER46, VAL35, and PHE39) surrounded ATR II with the lowest binding energy of -7.094Kcal/mol gained (fig. 5C).

DISCUSSION

A previous study reported that ATR II could be a novel chemopreventive agent in breast cancer; however, their study was limited to using human mammary epithelial MCF 10A cell line (Wang *et al*., 2017). In this study, ATR II was used to observe the signal transduction of NF-κB and the inhibitory effect of estrogen receptors (ERs) in breast cancer cells. The rationale for targeting the NF-κB ER pathway as a therapeutic target is that decreased levels of activated NF-κB have been observed in many human breast tumors. Likewise, compare to our previous studies (Wang *et al*., 2018). It can be clarified from these results that ATR stimulated the maximum cytotoxicity against human breast malignant and benign cancer cells with

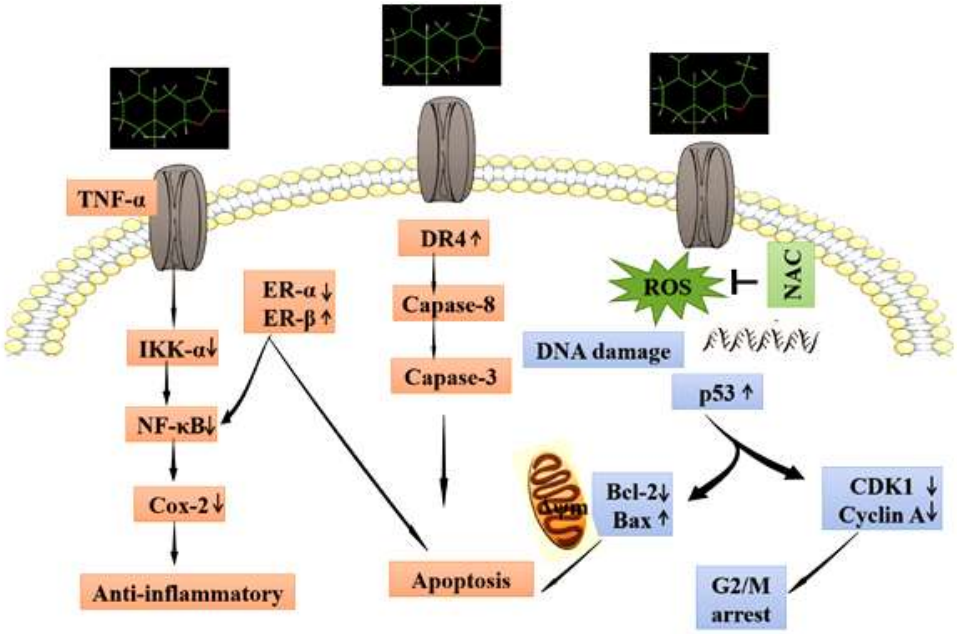

Fig. 6: Hypothetical mechanism of cytotoxicity mediated by ATR II on Breast cancer cells: ATR induces apoptosis by activated death receptor DR4, which results in the apoptosis of breast cancer through extrinsic pathways. Moreover, ATR II also induces oxidative stress, which might induce mitochondrial membrane collapse and promote in MCF-7 and MDA-MB 231 cells apoptosis and cell cycle arrest G2/M phase. On the other hand, ATR also might induce Breast cancer cell apoptosis by inhibiting inflammatory factors such as TNF-α, Cox2, and NF-KB that result in the inhibition of ER-α with over expression of ER-β, consequently drives the cells to their death by apoptosis.

lower drug concentrations. In contrast, ATR II does not have a significant effect on the normal breast cell line.

The interactive correlation between estrogen and ER-α has been found to help in breast cancer therapy (van Duursen *et al*. 2013). In contrast, although *in vivo* studies insist that ER-β could prohibit cell proliferation and cell cycle arrest based on its cancer suppression attributes, the relationship between estrogen and ER-β remains uncertain. Therefore, this study predicts ER-β expression in breast cancer cells, according to the ATR II-induced anti-proliferation activity. For ER-positive cells (MCF-7), it is feasible to add ATR II to improve ERβ concentration. Alternatively, ERβ expression in ER-negative MDA-231 cells will never be increased. Thus, it can be concluded that ATR II could trigger ERβ expression and prohibit cell proliferation. It undoubtedly affirms the relationship between phytoestrogen and ERβ in breast cancer cells.

Previous studies showed that ATR II retains antioxidant properties (Hoang le *et al*. 2016; Sumino *et al*. 2015). To elucidate whether ATR II can stimulate apoptosis of human breast cancer cells, flow cytometry for ROS was performed to evaluate the generation of hydrogen peroxide in MCF-7 and MDA-MB 231 cells. Our study showed that ATR II could produce H_2O_2, which can be reversed in NAC's presence. However, studies have already proven that the generation of ROS is interrelated with improved cell apoptosis. These results confirmed the antioxidant property of ATR II against human breast cancer MCF-7 and MDA-MB 231 cells.

Moreover, ROS was reported to promote and de-regulate mitochondrial membrane depolarization (Zareba and Palka 2016). Besides, targeting mitochondria was a novel approach for cancer therapy because of its involvement in stimulating apoptosis. In this regard, mitochondrial-mediated apoptosis can be highly regulated by counterbalancing the expressions of pro-apoptotic as well as anti-apoptotic proteins in the Bcl-2 proteins.

Nuclear factor NF-κB plays an essential role in developing breast cancer cell sensitivity to chemotherapeutics and radiotherapy. Besides, NF-κB plays a significant role in the inflammatory-mediated action of cell death by apoptosis. For instance, the human breast cancer cell line MCF-7 could not grow if inhibition of the NF-κB pathway (Kung *et al*. 2014; Thabet and Moustafa 2017). NF-κB remains in the cytoplasm in an inactive form through the regulation of IKK. The phosphorylation of IKK by TNF-α induces ubiquitination and degradation of IκB, which results in the translocation of NF-κB to the nucleus and subsequently initiates cell death (Ivanov *et al*. 2011). Our studies observed that ATR II inhibited the inflammatory factors COX-2, TNF-α, and NF-κB. We thus propose that ATR II treatment may result in the inhibition of NF-κB in MCF-7 and MDA-MB 231 cells as well, independent of their ER expression, which might be due to the phosphorylation of COX-2.

The cell cycle is the anatomical and physiological unit of life. The cell is the unit of the biological community for multicellular organisms. From that place, cell fulfills all the characteristics of living things, namely, functional organization, metabolism, homeostasis, growth and development, reproduction, passing on genetic information, responding to environmental changes, and ability to adapt through evolution. Cell cycle regulation plays a crucial role in cell death. Every phase of the cell cycle is regulated by cyclin's interaction and their relevant cyclin depend-kinases (CDK), which guaranteed one step to another. For instance, CDK1 could bind to cyclin-A G2/M transition (Jin *et al*. 2015; Liu *et al*. 2016). The CDK/cyclin complex activity is negatively regulated to induce cell cycle arrest by a p53-dependent or p53-independent pathway. In the p53-dependent pathway, the DNA-induced CDK inhibitor p21 increases in DNA-damaged cells with cell cycle arrest. Then non-repaired cells may be eliminated by apoptosis via inducing Bax and repressing Bcl-2 activity (Jin *et al*. 2015). Our data show that ATR II-induced MCF-7 and MDA-MB 231 cell accumulation in the G2/M phase. These results suggest that ATR II-mediated cell cycle arrest is followed by apoptosis. Western blot analysis showed that ATR II increased the expression of p53 and p21, a CDK inhibitor, which led to G2/M arrest. These results suggested that ATR II-mediated G2/M arrest occurs by inhibiting the CDK1/cyclinA complex via p53-dependent p21 induction.

CONCLUSION

Our findings highlight (fig. 6) the mitochondrial anti-proliferative role and pro-apoptotic role of ATR II in breast cancer cells. ATR II was found to trigger oxidative stress, inducing mitochondrial membrane collapse and promoting apoptosis in MCF-7 and MDA-MB 231 cells. In contrast, ATR II drives the activation of DR4 and promotes extrinsic apoptosis signaling. Furthermore, ATR II-mediated apoptosis in breast cancer cells is mainly mediated by inhibiting the inflammatory factor that leads to the estrogen receptor regulation. Simultaneously, ATR II causes breast cancer cell proliferation arrest at G2/M by inhibiting the CDK1/CyclinA complex and overexpression of the p53/p21complex.

ACKNOWLEDGEMENT

The present study was supported by 1. Tibet Autonomous Region Science and Technology Project XZ201801NB-11.

REFERENCES

Ashour F, Awwad MH, Sharawy HEL and Kamal M (2018). Estrogen receptor-positive breast tumors resist chemotherapy by the overexpression of P53 in Cancer Stem Cells. *J. Egypt Natl. Canc. Inst.,* **30**(2): 45-48.

Balhouse BN, Patterson L, Schmelz EM, Slade DJ, and Verbridge SS (2017) N-(3-oxododecanoyl)-L-homoserine lactone interactions in the breast tumor microenvironment: Implications for breast cancer viability and proliferation in vitro. *PLoS One.*, **12**(7): e0180372.

Bray F, Ferlay J, Soerjomataram I, Siegel RL, Torre LA and Jemal A (2018). Global cancer statistics 2018: GLOBOCAN estimates of incidence and mortality worldwide for 36 cancers in 185 countries. *CA Cancer J. Clin.,* **68**(6): 394-424.

Currey A, Patten CR, Bergom C, Wilson JF and Kong AL (2018). Management of the axilla after neoadjuvant chemotherapy for breast cancer: Sentinel node biopsy and radiotherapy considerations. *Breast J.,* **24**(6):902-910.

De Luca A, Fiorillo M and Peiris-Pages M, Bela O, Duncan L, Rosa S, Ubaldo E, Anna Rita C , Vincenzo P, Michael P and Federica S (2015) Mitochondrial biogenesis is required for the anchorage-independent survival and propagation of stem-like cancer cells. *Oncotarget.*, **6**(17): 14777-14795.

Dondelinger Y, Jouan-Lanhouet S and Divert T, Bela O, Duncan L, Rosa S, Ubaldo E, Anna Rita C, Vincenzo P, Michael P, Federica S, Theatre E, Bertin J, Gough Peter J, Giansanti P, Heck Albert JR, Dejardin E, Vandenabeele P and Bertrand Mathieu JM (2015). NF-kappa B-independent role of IKKalpha/IKKbeta in preventing RIPK1 kinase-dependent apoptotic and necroptotic cell death during TNF signaling. *Mol. Cell.,* **60**(1): 63-76.

Fengjiao J, Zhaozhen W, Xiao H, Jiahui Z, Zihe G, Xiao H, Junfang Q , Chen L and Yue W (2019). The PI3K/Akt/GSK-3β/ROS/eIF2B pathway promotes breast cancer growth and metastasis via suppression of NK cell cytotoxicity and tumor cell susceptibility. *Cancer Biol. Med.,* **16**(1): 38-54.

Hoang le S, Tran MH, Lee JS, Ngo QM, Woo MH and Min BS (2016). Inflammatory inhibitory activity of sesquiterpenoids from atractylodes macrocephala Rhizomes. *Chem. Pharm. Bull* (Tokyo), **64**(5):507-511.

House CD, Grajales V, Ozaki M, Jordan E, Wubneh H, Kimble DC, James JM, Kim MK and Annunziata CM (2018). IKappaKappaepsilon cooperates with either MEK or non-canonical NF-kB driving growth of triple-negative breast cancer cells in different contexts. *BMC Cancer,* **18**(1): 595.

Ivanov VN, Ghandhi SA, Zhou H, Huang SX, Chai Y, Amundson SA and Hei TK (2011). Radiation response and regulation of apoptosis induced by a combination of TRAIL and CHX in cells lacking mitochondrial DNA: A role for NF-kappaB-STAT3-directed gene expression. *Exp. Cell. Res.,* **317**(11): 1548-1566.

Jin S, Park HJ, Oh YN, Kwon HJ, Kim JH, Choi YH and Kim BW (2015). Anti-cancer activity of osmanthus matsumuranus extract by inducing G2/M

arrest and apoptosis in human hepatocellular carcinoma Hep G2 Cells. *J. Cancer Prev.,* **20**(4): 241-249.

Kalyanaraman B, Cheng G, Hardy M, Ouari O, Bennett B and Zielonka J (2018). Teaching the basics of reactive oxygen species and their relevance to cancer biology: Mitochondrial reactive oxygen species detection, redox signaling, and targeted therapies. *Redox Biol.,* **15**: 347-362

Kung G, Dai P, Deng L and Kitsis RN (2014). A novel role for the apoptosis inhibitor ARC in suppressing TNF alpha-induced regulated necrosis. *Cell Death Differ.,* **21**(4): 634-44.

Lin F, Lei S, Ma J, Shi L, Mao D, Zhang S, Huang J, Liu X, Ding D, Zhang Y and Zhang S (2016). Inhibitory effect of jianpi-jiedu prescription-contained serum on colorectal cancer SW48 cell proliferation by mTOR-P53-P21 signalling pathway. *Zhong Nan Da Xue Xue Bao Yi Xue Ban.,* **41**(11): 1128-1136.

Liu KC, Shih TY, Kuo CL, Ma YS, Yang JL, Wu PP, Huang YP, Lai KC and Chung JG (2016). Sulforaphane induces cell death through G2/M phase arrest and triggers apoptosis in HCT 116 human colon cancer cells. *Am. J. Chin. Med.,* **44**(6): 1289-1310.

Losada-Echeberria M, Herranz-Lopez M, Micol V and Barrajon-Catalan E (2017). Polyphenols as promising drugs against main breast cancer signatures. *Antioxidants (Basel).,* **6**(4):88.

Nasser MI, Han T, Adlat S, Tian Y and Jiang N (2018). Inhibitory effects of Schisandrin B on human prostate cancer cells. *Oncol. Rep.,* **41**(1):677-685

Nasser MI, Masood M, Wei W, Xiaochun L, Yifa Z, Bao L, Jiang Li, Xiaomeng (2017). Cordycepin induces apoptosis in SGC7901 cells through mitochondrial extrinsic phosphorylation of PI3K/Akt by generating ROS. *Int. J. Oncol.,* **50**(3): 911-919.

Park C and Lee Y (2014). Overexpression of ER beta is sufficient to inhibit hypoxia-inducible factor-1 transactivation. *Biochem. Biophys. Res. Commun.,* **450**(1): 261-266.

Ponde NF, Zardavas D and Piccart M (2018). Progress in adjuvant systemic therapy for breast cancer. *Nat. Rev. Clin. Oncol.,* **16**(1): 27-44.

Qi C, Zhu YT, Chang J, Yeldandi AV, Rao MS and Zhu YJ (2005). Potentiation of estrogen receptor transcriptional activity by breast cancer amplified sequence 2. *Biochem. Biophys. Res. Commun,* **328**(2): 393-398.

Quintela-Fandino M, Soberon N and Lluch A, Manso L, Calvo I and Cortes J (2017). Critically short telomeres and toxicity of chemotherapy in early breast cancer. *Oncotarget.,* **8**(13): 21472-21482.

Samin M , Behzad J, Parina A, Miquel M and Javad S (2020). Medicinal plants used in the treatment of Malaria: A key emphasis to Artemisia, Cinchona, Cryptolepis, and Tabebuia genera. *Phytother Res.,* **34**(7):1556-1569**.**

Shrivastava S, Kulkarni P, Thummuri D, Jeengar MU, Naidu VGM, Alvala M, Redddy GB and Ramakrishna S (2014). Piperlongumine, an alkaloid causes inhibition of PI3 K/Akt/mTOR signaling axis to induce caspase-dependent apoptosis in human triple-negative breast cancer cells. *Apoptosis,* **19**(7): 1148-1164.

Sumino M, Saito Y, Ikegami F and Namiki T (2015). A simultaneous determination of principal compounds in tokishakuyakusan by high-performance liquid chromatography with diode array detector. *J. Chromatogr. Sci.,* **53**(2): 320-324.

Sun Z, Zhou D, Xie X, Wang S, Wang Z, Zhao W, Xu H and Zheng L (2016). Cross-talk between macrophages and atrial myocytes in atrial fibrillation. *Basic. Res. Cardiol.,* **111**(6): 63.

Szmyd M, Lloyd V, Hallman K, Aleck K, Mladenovik V, McKee C, Morse M, Bedgood T and Dinda S (2018). The effects of black cohosh on the regulation of estrogen receptor (ERalpha) and progesterone receptor (PR) in breast cancer cells. *Breast Cancer (Dove Med Press),* **10**: 1-11

Thabet NM and Moustafa EM (2017). Synergistic effect of Ebselen and gamma radiation on breast cancer cells. *Int. J. Radiat Biol.,* **93**(8):784-792.

Tian S and Yu H (2017). Atractylenolide II inhibits proliferation, motility and induces apoptosis in human gastric carcinoma cell lines HGC-27 and AGS. *Molecules,* **22**(11): 1886.

Van Duursen MB, Smeets EE, Rijk JC, Nijmeijer SM and van den Berg M (2013). Phytoestrogens in menopausal supplements induce ER-dependent cell proliferation and overcome breast cancer treatment in an in vitro breast cancer model. *Toxicol Appl Pharmacol.,* **269**(2): 132-140.

Wang J, Nasser MI, Adlat S, Ming Jiang M, Jiang N and Gao L (2018). Atractylenolide II induces apoptosis of prostate cancer cells through regulation of AR and JAK2/STAT3 signaling pathways. *Molecules,* **23**(12): 3298.

Wang T, Long F, Zhang X, Yang Y, Jiang X and Wang L (2017). Chemopreventive effects of atractylenolide II on mammary tumorigenesis via activating Nrf2-ARE pathway. *Oncotarget*, **8**(44): 77500-77514.

Xiao L, Luo Y, Tai R, and Zhang N (2019) Estrogen receptor beta suppresses inflammation and the progression of prostate cancer. *Mol. Med. Rep.,* **19**(5): 3555-3563.

Ye Y, Wang H, Chu JH, Chou GX, Chen SB, Mo H, Fong WF and ZL Y (2011). Atractylenolide II induces G1 cell-cycle arrest and apoptosis in B16 melanoma cells. *J. Ethnopharmacol.,* **136**(1): 279-82.

Yim NH, Gu MJ, Park HR, Hwang YH and Ma JY (2018). Enhancement of neuroprotective activity of Sagunja-tang by fermentation with lactobacillus strains. *BMC Complement Altern Med.,* **18**(1): 312.

Zareba I and Palka J (2016). Prolidase-proline dehydrogenase/proline oxidase-collagen biosynthesis axis as a potential interface of apoptosis/autophagy. *Biofactors.,* **42**(4): 341-348.